



Available online at www.sciencedirect.com

SCIENCE @ DIRECT®

C. R. Chimie 9 (2006) 301–306



<http://france.elsevier.com/direct/CRAS2C/>

Preliminary communication / Communication

Electrochromic and photoelectrochemical characteristics of nanostructured WO₃ films prepared by a sol–gel method

Renata Solarska, Bruce D. Alexander, Jan Augustynski *

Département de chimie minérale, analytique et appliquée, université de Genève, quai Ernest-Ansermet 30, 1211 Genève, Switzerland

Received 22 July 2004; accepted after revision 26 November 2004

Available online 09 September 2005

Abstract

The preparation of mesoporous tungsten trioxide from tungstic acid and tungstic hexaethoxide precursors containing an added organic stabiliser via a sol–gel method is reported. The effect of annealing temperature and precursor species on the photoelectrochemical performance and the electrochromic colouration efficiencies has been discussed with the help of the characterisation of crystalline structure (through Raman microscopy) and surface morphology (through SEM imaging). *To cite this article: R. Solarska et al., C. R. Chimie 9 (2006).*

© 2005 Académie des sciences. Published by Elsevier SAS. All rights reserved.

Résumé

La préparation du trioxyde de tungstène mésoporeux par la méthode sol–gel à partir des deux précurseurs – l'acide tungstique et le hexaéthoxyde de tungstène – contenant un stabilisateur organique est décrite. L'effet de la température du traitement thermique et de la nature du précurseur sur la photoélectrochimie et l'électrochromisme des films de WO₃ est présenté, en relation avec leur structure cristalline (microscopie Raman) et la morphologie (MEB). *Pour citer cet article : R. Solarska et al., C. R. Chimie 9 (2006).*

© 2005 Académie des sciences. Published by Elsevier SAS. All rights reserved.

Keywords: Photoelectrochemistry; Electrochromism; WO₃; Thin films; Raman spectroscopy; Sol–gel synthesis

Mots clés : Photoélectrochimie ; Électrochromisme ; WO₃ ; Couches minces ; Spectroscopie Raman ; Synthèse sol–gel

1. Introduction

Given the substantial number of potential applications for microporous and mesoporous oxide films (het-

erogeneous catalysis, photonic and electrocatalytic materials, sensors, batteries, etc.) it should not be surprising that the controlled production of such films has attracted a great deal of attention [1–3]. Thin films of metal oxides may be prepared by a number of means, although it is perhaps the sol–gel method, which offers the greatest possibility of controlling film morphology

* Corresponding author.

E-mail address: jan.augustynski@chiam.unige.ch (J. Augustynski).

and porosity owing to the numerous experimental parameters, which may be varied, such as choice of precursor and processing conditions.

Furthermore, it may be possible to induce structural ordering in the oxide films during the heat-treatment process by the addition of a structure-directing agent into either the sol or the gel. Unfortunately, the high-temperature heat treatments often required to form well-crystallised films have a tendency to collapse such template-mediated, ordered mesostructures. Therefore, a compromise must be reached between conditions suitable for the formation of mesopores and those for producing a well-crystallised film.

We have recently described the synthesis of such well-crystallised mesoporous WO₃ films [4]. Such films exhibit particularly promising photoelectrochemical properties, especially for the development of efficient photoanodes for water splitting under visible light illumination. Indeed, WO₃ may be regarded as an improvement on other materials, such as TiO₂, as the photoreponse extends into the blue region of the solar spectrum, up to 500 nm. Furthermore, photocurrent densities for the photoelectrolysis of water, recorded in acidic solutions under AM 1.5 irradiation, have been reported to reach 3 mA cm⁻² [5].

Another possible application of thin films of WO₃ is in electrochromic devices due to their open and porous structure, which is a consequence of their nanocrystalline nature. These films combine excellent transparency to longer wavelengths than 550 nm with short diffusion paths for intercalating cations (Li⁺, H⁺). In this communication, we report the changes in structure and morphology of WO₃ films upon variation of processing conditions. A connection shall be made with the observed changes in photoelectrochemical and electrochromic properties of the WO₃ films and their structure and morphology as monitored by Raman microscopy and SEM.

2. Materials and methods

Precursor solutions consisted of either freshly prepared tungstic acid or anhydrous tungsten (VI) ethoxide, 5% w/w ethanol (Alfa Aesar). Poly(ethylene glycol) 300 (PEG) was added to these solutions, such that the PEG/WO₃ ratio was of the order of 0.5 w/w. The

WO₃ films were prepared by spreading a small quantity of the precursor solution onto a conducting glass substrate (0.5- μ m F-doped SnO₂ overlayer, Nihon Sheet Glass Co., 12 Ω sq⁻¹). After drying at room temperature for 10 min, the WO₃ films were annealed in flowing oxygen for 30 min between 250 and 550 °C.

The crystallinity of the samples was analysed by Raman microscopy using a LabRam I confocal Raman microscope. A frequency-doubled Nd:YAG laser provided excitation at 532.0 nm. In order to minimise photodegradation of the sample, the power was between 25 and 110 μ W, depending on the sample. Spectra recorded from a number of positions on the surface were found to be highly reproducible. UV–vis transmission spectra were recorded on a Perkin–Elmer, Lambda 900 spectrophotometer. The morphology of the samples was examined using a LEO Gemini 982 scanning electron microscope (SEM) equipped with a Röntec energy dispersive X-ray analysis (EDX) detector system.

Electrochromic experiments were performed in either a solution of 1 M LiClO₄ in anhydrous propylene carbonate or 1 M aqueous H₂SO₄ using electrodes consisting of 0.4 μ m-thick WO₃ films. The photoelectrochemical activity was tested in a 3 M H₂SO_{4(aq)} solution by illuminating the WO₃ electrode from the side of the electrolyte/film interface in a Teflon cell. WO₃ electrodes were illuminated with simulated solar AM 1.5 light, obtained using a 150-W xenon lamp fitted with a Schott 113 filter and neutral density filters. The cell was fitted with a quartz window and the counter and reference electrodes were a Pt foil and a saturated calomel electrode (SCE), respectively. The wavelength photoresponse (i.e. quantum efficiency of the photocurrent vs. excitation wavelength) of the electrodes was determined using a 500-W xenon lamp (Ushio UXL-502HSO) set in an Oriel model 66021 housing and a Multispec 257 monochromator (Oriel) with a typical bandwidth of 4 nm. The intensity of the incident light from the monochromator was measured using a model 730 A radiometer/photometer (Optronic Lab). All solutions were prepared with analytical grade reagents and Milli-Q water and were thoroughly degassed with nitrogen prior to measurement. Photoelectrochemical and electrochromic measurements were carried out under potential-controlled conditions using an EG&G Princeton Applied Research Model 362 potentiostat.

3. Results and discussion

3.1. Characterisation

The effect of annealing the thin films of WO_3 over a range of temperatures upon the crystalline structure has been monitored by Raman microscopy, shown in Fig. 1. The spectra of the WO_3 films produced following annealing at 350 and 400 °C, Fig. 1(a) and 1(b), respectively, are very similar. Indeed, the primary difference between the two films is the reduction in carbon content brought about by annealing at the higher temperature. Nonetheless, the combustion of PEG is not complete even at 400 °C, as evidenced by the presence of a weak broad band at ca. 1600 cm^{-1} . The band present at 962 cm^{-1} in both Fig. 1a and b is typical of $\nu(\text{W}=\text{O})$ and is attributed to terminal $\text{W}=\text{O}$ groups, such as those present in hydrated forms of tungsten oxides [6,7]. The strong broad feature comprising a band at 780 cm^{-1}

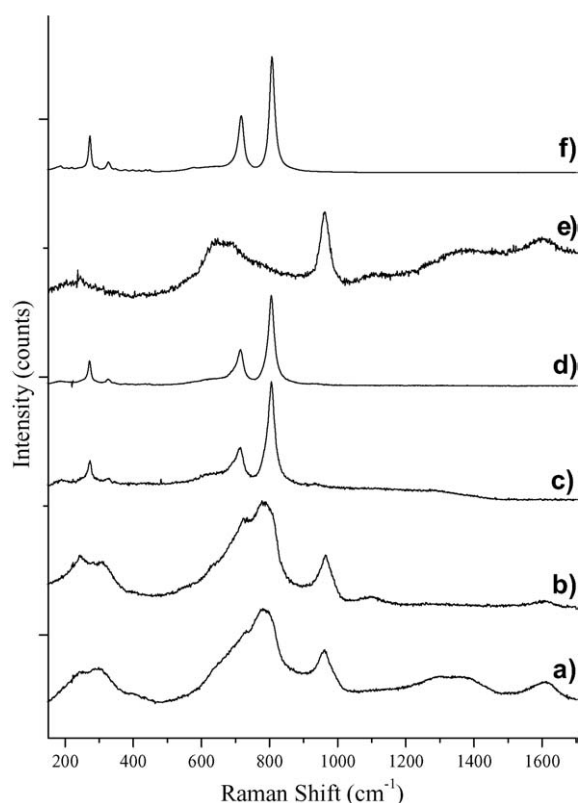


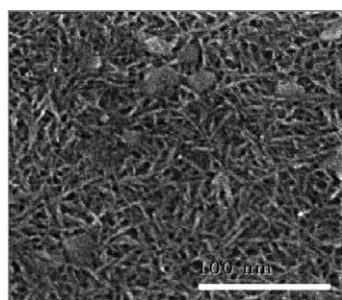
Fig. 1. Raman spectra of WO_3 films derived from tungstic acid precursor annealed at (a) 350 °C; (b) 400 °C; (c) 500 °C and (d) 550 °C. Raman spectra of WO_3 films formed from tungstic hexaethoxide precursor annealed at (e) 500 °C; and (f) prolonged annealing at 550 °C.

and a shoulder at 732 cm^{-1} is due to $\nu(\text{W}-\text{O})$ involving the oxygen atoms bridging neighbouring octahedra. These features closely resemble those of amorphous WO_3 , although the presence of a trace amount of the hexagonal phase of WO_3 cannot be ruled out for films annealed at 400 °C [8]. The shoulder at 635 cm^{-1} may be ascribed to h- WO_3 , and it is possible that the band previously observed in h- WO_3 at 817 cm^{-1} [7] may be obscured by the broad hydrate band in Fig. 1b.

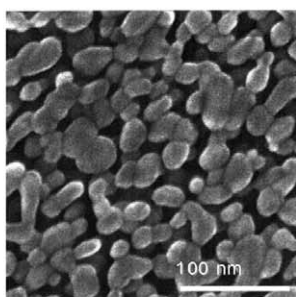
A dramatic change in crystalline structure is observed upon raising the annealing temperature to 500 °C, as evidenced by the complete transformation of the Raman spectrum, shown in Fig. 1c. Critically, the $\nu(\text{W}=\text{O})$ band at 963 cm^{-1} disappears upon raising the annealing temperature, indicating a removal of terminal oxygen atoms. Indeed, the spectra of the WO_3 films annealed at 500 and 550 °C, shown in Fig. 1c and d, display well-defined bands at 271, 723 and 805 cm^{-1} , which can be easily assigned to the $\delta(\text{O}-\text{W}-\text{O})$ and $\nu(\text{W}-\text{O})$ bands of monoclinic WO_3 [7]. Furthermore, the combustion of the organic additive appears to be complete due to the lack of bands attributable to carbonic species between 1300 and 1630 cm^{-1} . A significant increase in the signal-to-noise ratio is observed on increasing the annealing temperature from 500 to 550 °C, with the latter being at least twice as strong, thereby indicating a substantial increase in crystallinity of the monoclinic phase.

Thin films have also been prepared using tungstic hexaethoxide. Fig. 1e shows the Raman spectrum of a tungstic hexaethoxide-produced WO_3 film annealed at 500 °C; the difference upon comparison with its tungstic acid-derived equivalent is pronounced. Notwithstanding the presence of carbon bands in Fig. 1e, even after annealing at 500 °C the film produced from the tungstic hexaethoxide precursor shows no appreciable crystallinity. A large quantity of terminal $\text{W}=\text{O}$ groups are present, as indicated by the strong band at 961 cm^{-1} . This band, along with the overlapping bands at 648 and 685 cm^{-1} , are similar to those found in the Raman spectrum of $\text{WO}_3 \cdot 2 \text{H}_2\text{O}$ [7]. After prolonged annealing at 550 °C, the Raman spectrum, Fig. 1f, shows the clear formation of monoclinic WO_3 accompanied by the complete removal of any carbonic species.

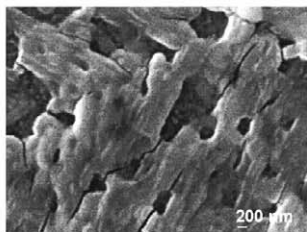
From the micrographs shown in Fig. 2, it can be seen that the morphology of WO_3 films is also dependent on the annealing temperature and the choice of precursor. Films produced from tungstic acid/PEG and annealed



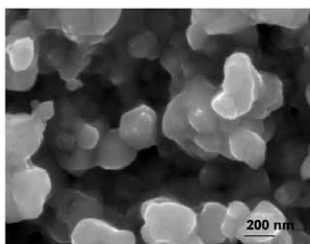
a)



b)



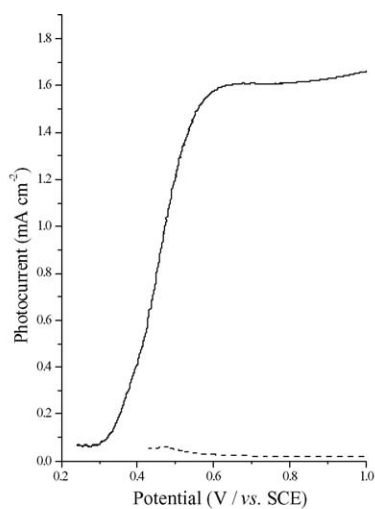
c)



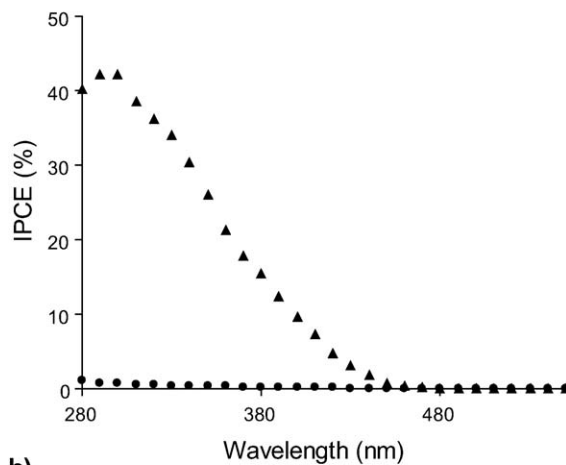
d)

Fig. 2. Scanning electron micrographs of films formed from (a) tungstic acid precursor, annealed at 400 °C; (b) tungstic acid precursor, annealed at 500 °C; (c) tungsten (VI) ethoxide precursor annealed at 500 °C and (d) tungsten (VI) ethoxide precursor annealed at 300 °C followed by additional annealing at 550 °C.

at 400 °C (Fig. 2a) show a dense network of needle-like particles, which are ca. 30 nm long. After annealing at 500 °C (Fig. 2b), these needle-like particles are replaced by a porous film consisting of spherical features of 10–25 nm diameter. In comparison, WO_3 films annealed at 500 °C prepared from the tungstic hexaethoxide/PEG precursor (Fig. 2c) display a considerable degradation in porosity. An array of rectangular 300 × 1000-nm plate-like features is observed. Such a lack of porosity is thought to be due to the



a)



b)

Fig. 3. (a) Photocurrent-potential curve of ca. 0.4- μm -thick WO_3 films prepared from tungstic acid/PEG precursor annealed at 400 °C (dashed lines) and 500 °C (solid line) recorded at 50 mV s^{-1} in 3 M $\text{H}_2\text{SO}_4(\text{aq})$ under 1 sun AM 1.5 illumination. (b) IPCE of ca. 0.4- μm -thick WO_3 films prepared from tungstic acid/PEG precursor annealed at 400 °C (solid circles) and 500 °C (solid triangles). Electrodes were polarised at 1.0 V vs. SCE.

residual organic species, as shown in Fig. 1e. After annealing at 550 °C, a substantial increase in porosity is observed (Fig. 2d), accompanied by the appearance of 200-nm diameter spherical surface features: these features are substantially larger than those of the WO₃ films prepared from the tungstic acid/PEG precursor.

3.2. Photoelectrochemistry

Photocurrents were measured in 3 M H₂SO₄ under 1 sun irradiation (Fig. 3a), and show a marked dependence upon the temperature at which the films were annealed. At annealing temperatures below 500 °C, the WO₃ films afforded photocurrents of only 0.05 mA cm⁻². Films produced after annealing at 500 °C show a dramatic improvement in the photocurrent, which reaches 1.60 mA cm⁻² for these 0.4-μm-thick films. A similar dependence on annealing temperature is observed in the spectral responses. From Fig. 3b, it can be seen that the incident photon-to-current conversion efficiencies, IPCEs, for WO₃ films annealed at 400 °C are generally less than 1%. Annealing at 500 °C affords IPCEs of 45% with a maximum at ca. 300 nm. This is clearly linked to the formation of monoclinic WO₃ at annealing temperatures above 500 °C, as observed by Raman microscopy. Further improvements in photocurrents and IPCEs may be gained upon increasing the thickness of the films.

3.3. Electrochromism

Fig. 4 displays the transmittance spectra of the WO₃ films annealed at 500 °C in both their natural state and

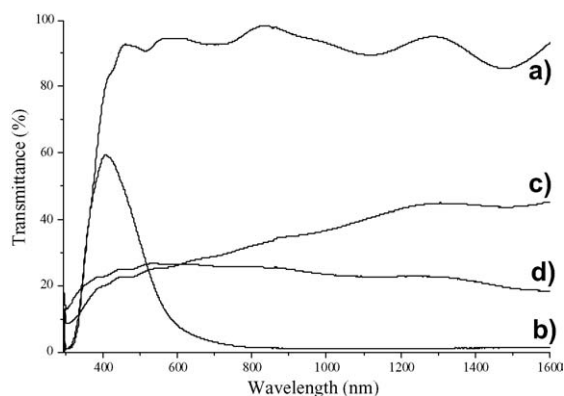


Fig. 4. Transmittance spectra of WO₃ films annealed at 500 °C. Spectra (a) natural and (b) coloured WO₃ films prepared from tungstic acid/PEG precursor. Spectra (c) natural and (d) coloured WO₃ films prepared from tungstic hexaethoxide/PEG precursor.

coloured state following H⁺ insertion. Following H⁺ insertion, the transmittance of the film produced from a tungstic acid precursor at wavelengths longer than 600 nm changes from 90% to less than 10% (Fig. 4a and b). Furthermore, the performance of these films was found to be stable when subjected to continual colouration–bleaching cycles in H₂SO_{4(aq)} for an extended period of time, thus indicating the good chemical and mechanical stability of the films. By comparison, the tungstic hexaethoxide-derived films display a much smaller change in transmittance. Furthermore, these films are not transparent, unlike those prepared from tungstic acid. Tungstic hexaethoxide-prepared films have a cloudy appearance in their bleached state and exhibit a bluishness upon colouration. In order to evaluate the electrochromic performance of these films, the colouration efficiency (CE), has been recorded for both Li⁺ (Fig. 5) and H⁺ insertion (not shown). Colouration efficiency is defined as:

$$CE = \frac{\Delta OD}{q} \quad (1)$$

i.e. the change in optical density, OD, with respect to the amount of charge inserted, *q*. The CEs shown in Fig. 5 are increased compared to those normally observed. For example, a CE of 66 cm² C⁻¹ has been reported for a film annealed at 300 °C [9], while a CE of 40 cm² C⁻¹ has been reported for a film annealed at 500 °C [4]. In the present case, it is the response of the CEs to the annealing temperature that is interesting.

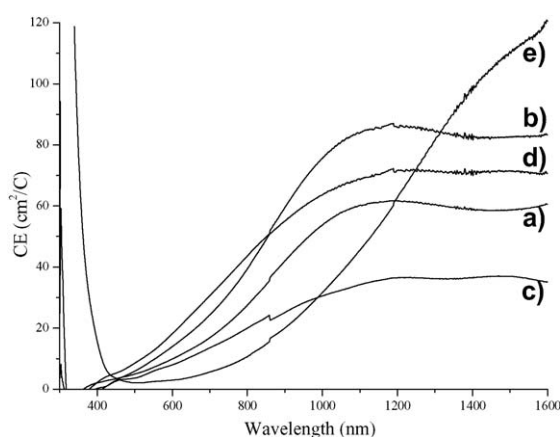


Fig. 5. Colouration efficiency (CE) of WO₃ films prepared from tungstic acid/PEG precursor in 1 M LiClO₄ in propylene carbonate solutions as a function of annealing temperature. (a) 250 °C; (b) 300 °C; (c) 350 °C; (d) 400 °C and (e) 500 °C.

Above 1300 nm, the film annealed at 500 °C displays the largest colouration efficiencies, followed by the film annealed at 300 °C. Indeed, for H⁺ insertion, the CE of the film annealed at 500 °C is larger than those of the other films throughout the entire spectral range. The ordering may arise from two factors: porosity and crystal phase. Films of higher porosity tend to give higher CEs. Note that the largest porosity was observed for films annealed at 500 °C. Crystal phase may also be a determining factor as, for example, amorphous WO₃ has been shown to be an excellent electrochromic material [10]. The Raman spectra indicate that as the amount of amorphous WO₃ decreases, there is a concomitant increase in hexagonal WO₃ (which may be considered to be unfavourable for the electrochromic behaviour). The CE decreases along with the amount of amorphous WO₃, until the highly porous monoclinic WO₃ is formed at 500 °C.

4. Conclusions

Mesoporous thin films of WO₃ were prepared following a sol–gel method involving the addition of an organic structure-directing agent to a tungstic acid, or tungstic hexaethoxide precursor. The effect of the choice of precursor and annealing temperature were investigated. Well-crystallised WO₃ films were formed which combine good adherence and mechanical stability with the high photoelectrochemical and electrochromic performance. These observations, have been found

to be linked to variations in crystal phase of WO₃ and the surface morphology. The presence of monoclinic WO₃ is essential to obtain good photoelectrochemical properties of the films.

Acknowledgements

This work was supported by the Swiss National Science Foundation and the Swiss Federal Office of Energy.

References

- [1] C.T. Kresge, M.E. Leonowicz, W.J. Roth, J.C. Vartuli, J.S. Beck, *Nature* 359 (1992) 710.
- [2] Z. Tian, W. Tong, J. Wang, N. Duan, V.V. Krishnan, S.L. Suib, *Science* 276 (1997) 926.
- [3] P. Yang, D. Zhao, D.I. Margolese, B.F. Chmelka, G.D. Stucky, *Nature* 396 (1998) 152.
- [4] C. Santato, M. Odziemkowski, M. Ulmann, J. Augustynski, *J. Am. Chem. Soc.* 123 (2001) 10639.
- [5] C. Santato, M. Ulmann, J. Augustynski, *J. Phys. Chem. B* 105 (2001) 936.
- [6] K. Nonaka, A. Takase, K. Miyakawa, *J. Mater. Sci. Lett.* 12 (1993) 274.
- [7] M.F. Daniel, B. Desbat, J.C. Lassegues, B. Gerand, M. Figlarz, *J. Solid-State Chem.* 67 (1987) 235.
- [8] S. Lee, H.M. Cheong, C.E. Tracy, A. Mascarenhas, D.K. Benson, S.K. Deb, *Electrochim. Acta* 44 (1999) 3111.
- [9] Y. Djaoued, P.V. Ashrit, S. Badilescu, R. Brüning, *J. Sol–Gel Sci, Technol.* 28 (2003) 235.
- [10] S. Lee, H.M. Cheong, J. Zhang, A. Mascarenhas, D.K. Benson, S.K. Deb, *Appl. Phys. Lett.* 74 (1999) 242.